Journal of Crustacean Biology Advance Access published 18 December 2018

The Crustacean Society

Journal of Crustacean Biology

Journal of Crustacean Biology 39(3) 218–226, 2019. doi:10.1093/jcbiol/ruy088

Embryonic development of the myodocopid ostracod *Euphilomedes carcharodonta* Smith, 1952

Kristina H. Koyama and Ajna S. Rivera

Department of Biological Sciences, University of the Pacific, Stockton, CA 95211, USA

Correspondence: A.S. Rivera; e-mail: arivera@pacific.edu

(Received 1 April 2018; accepted 15 October 2018)

ABSTRACT

Pancrustaceans in general display a wide variety of developmental strategies and are morphologically diverse. The evolution of many compelling pancrustacean features, such as limbs and diverse nervous/sensory systems, however, are not well understood due to a lack of sampling across clades. Ostracods are representatives of the understudied, basally branching Oligostraca. While their amazing fossil record is well-characterized, little is known about the development of any oligostracan. We are developing *Euphilomedes carcharodonta* Smith, 1952 (Myodocopida, Sarsielloidea, Philomedidae) as a novel model for studying evolution and development within Ostracoda. We examined practical aspects including antibody staining, brood size, time course of embryogenesis, and artificial rearing, as well as provide a description of sarsielloid cell-division patterns, a broad description of the embryonic nervous system, limb bud, and developing carapace.

Key Words: carapace, Crustacea, DAPI, embryogenesis, embryology, evolutionary biology, germband, immunohistochemistry, juveniles, limbs, Ostracoda

EIGHTEENTH INTERNATIONAL SYMPOSIUM ON OSTRACODA

INTRODUCTION

While ostracods comprise a major pancrustacean class, their basic biology is understudied compared to other crustacean classes. The vast majority of species are known only from the fossil record, approximately 65,000 of the 95,000 known species are only described from fossils (Brusca *et al.*, 2016; Ikeya *et al.*, 2005). Because ostracods have a rich fossil record and are valuable indicator species, much of the focus of ostracod research has been on micropaleontology and biostratigraphy. Interest has recently grown on the biology of living ostracods, in particular in their bioluminescence, evolution, and behavior (e.g., Oakley, 2005; Rivers & Morin, 2013; Speiser, 2013; Ellis & Oakley, 2016; Gerrish & Morin, 2016; Arenz *et al.*, 2018). Possibly the least studied aspect of this understudied taxon is their embryology and juvenile development. This is a particularly weighty omission as ostracods are a diverse clade within the most basally branching group of Pancrustacea (Oligostraca; Oakley *et al.*, 2013) and could give clarity to the murky early evolution of this group. Ostracods themselves also have compelling features with unresolved developmental and evolutionary origins, for example their bivalved hinged carapace. Other characters, such as bioluminescent mucus, and sexually dimorphic eyes, have apparently each evolved multiple times (Oakley, 2005). Here we provide the first overview of embryogenesis of a sarsielloid (Myodocopida) ostracod and the first microphotographs of a developing ostracod nervous system.

Euphilomedes carcharodonta Smith, 1952 is a benthic ostracod found in the shallow subtidal off the Pacific coast of North America. Myodocopid ostracods, including *E. carcharodonta*, undergo direct development, with free-swimming juvenile instars which resemble small adults. Like other myodocopids, females of this species brood their eggs in a marsupium, a brood pouch within the female carapace, from which they hatch at the completion of embryogenesis and the beginning of the first juvenile stage, instar I (Cohen & Morin, 1990). They develop through four additional juvenile stages (instars II-V) before a final molting to an adult stage (Kornicker & Harrison-Nelson, 1997).

While the development of myodocopid ostracods has been studied previously, most studies have focused on the gross morphology of juvenile development (e.g., Turpen & Angell, 1971; Cohen, 1983; Baltanás *et al.*, 2000; Kornicker & Harrison-Nelson, 2002; Smith & Kamiya, 2002, 2005; Horne *et al.*, 2004), fewer have described macroscopic timeline events of embryogenesis (e.g. Gerrish & Morin, 2008) and only two studies have examined embryological processes in a myodocopid, the cypridinid *Vargula hilgendorfii* Mueller, 1890 (Wakayama, 2007; Ikuta, 2017). Wakayama (2007) examined nuclear stained (DAPI) embryos and made a timeline based on limb and carapace development. Ikuta

(2017) furthered this research by examining segmentation, especially significant as myodocopids are extremely oligosegmented arthropods. Both studies found that the five anteriormost limb buds, of a total of seven, appear simultaneously along with the carapace (Ikuta, 2017).

Our study expands what is already known about ostracod embryology by providing a protocol for immunohistochemical staining of an ostracod, the first detailed look at the embryology of a sarsielloid, and the first published microphotographs of the development of the ostracod nervous system. Our primary study species, *E. carcharodonta*, is simple to collect with inexpensive equipment, can be kept in small containers in a laboratory setting, and has large (relative to body size) embryos. They present a promising opportunity to explore the embryonic development of ostracods and add to the scarce knowledge on myodocopid development.

MATERIALS AND METHODS

Collection of Euphilomedes carcharodonta *embryos*

We collected *E. carcharodonta* from Pillar Point, Half Moon Bay, California as previously described (Sajuthi *et al.*, 2015). We collected sand approximately 10 m from shore with hand nets during low tide. The sand was sorted on site with sieves with 500 µm mesh to remove silt. We stored ostracods in sand in plastic 20 l buckets with an aquarium bubbler until sorting. Ostracods were sorted out of sand under a dissection microscope and separated by sex and approximate age into petri dishes containing artificial seawater. The dishes were then stored at 12–14 °C

We used a low power dissection microscope with top lighting to assess the presence and approximate stage of brooding females, using the color of embryos as an indication of age (see Supplementary material Fig. S1). To remove embryos, we placed a brooding female in a small petri dish with artificial seawater, and quickly cracked open the carapace with insect pins. We used the pins to gently move embryos into the dish.

Embryos were either maintained in 6-well plates in artificial seawater at 12–14 °C or fixed for staining in 4% paraformaldehyde in PBS (PFA). Adults were transferred into microcentrifuge tubes using forceps and embryos were transferred using a micropipette, taking care not to transfer excess seawater. Following an overnight fixation at 4 °C, animals were washed three times 30 min each in PBS.

Immunohistochemistry

We visualized the embryonic nervous system of *E. carcharodonta* using immunohistochemistry, with an antibody against acetylated alpha-tubulin using a modified crustacean staining protocol (e.g., Harzsch *et al.*, 1997; Harzsch & Glötzner, 2002; Brenneis & Richter, 2010; Brenneis *et al.*, 2013; Mayer *et al.*, 2013).

We pre-incubated fixed embryos in preparation for staining, as follows: NH_4Cl for 5 min, followed by 0.2% Triton-X in PBS for 10 min, followed by cold PBS for 5 min. Staining of embryos with antibodies required physical permeabilization of the chorion with a microneedle. We blocked embryos in a 0.1% BSA solution in 0.3% Triton-X in PBS for 1 h. We diluted the primary antibody (mouse anti-acetylated alpha tubulin; Sigma-Aldrich, Darmstadt, Germany) in blocking solution 1:20 and incubated at room temperature for 1 h. The following day, we washed embryos three times at 30 min each in PBS, then added the secondary antibody (FITC-conjugated goat anti-mouse IgG (ImmunoReagents, Raleigh, NC, USA) diluted 1:20 in blocking solution incubated overnight at 12 °C with shaking protected from light. Following immunostaining, embryos were counterstained in a DAPI/30% glycerol solution for at least 1 h prior to mounting in 70% glycerol. We confirmed our immunostaining results with phalloidin staining (data not shown). Phalloidin stains F-actin, which is abundant in developing arthropod axons (Harzsch *et al.*,1997). For embryos stained with DAPI alone, we washed fixed embryos three times 15 min each in PBS, then stained in DAPI/30% glycerol overnight at 4 °C.

For visualization under a compound microscope, we mounted animals on specially prepared agar slides in a preparation modified from methods used to visualize the nematode *Caenorhabditis elegans* (Walston & Hardin, 2010). We applied two layers of laboratory tape to standard glass microscope slides on either long edge and placed a drop of hot 2% agarose solution on the center of the slide. We flattened the hot drop of agarose by placing a second microscope slide on top. The agarose set until cool, and then we removed top microscope slide and tape to reveal a thin, even layer of agarose on the slide. We trimmed the edges using a razor blade and cut wells into the agar layer using a p200 micropipette tip.

To mount the embryos, we covered the agarose pad in a drop of 70% glycerol, placed the stained embryos into wells, and covered the slide with a coverslip. We were then able to rotate the embryos and reposition them in the wells by gently sliding the coverslip over the agarose pad. This allowed for microphotography of several angles of the embryo.

Microscopy and microphotography

We visualized fluorescently stained embryos using a compound LED microscope (Zeiss Axio Scope.A1, Oberkochen, Germany) and took color microphotographs with a Canon EOS Digital Rebel XS camera (Canon, Tokyo, Japan) at several depths of field for each specimen. We compiled images into stacks, then merged into composite images using ImageJ (ver. 1.50i; National Institutes of Health, Washington, DC, USA) stack and Z-projection functions (maximum intensity) and Helicon Focus (Heliconsoft, Kharkiv, Ukraine). We converted images to black and white 8-bit images for increased contrast because images were used for general reference and not for quantification.

We mounted live embryos, either freshly removed from the marsupium or artificially reared in wells (see below), in a large drop of seawater on a microscope slide and visualized them under a dissection microscope. Microphotographs were taken using a Canon EOS Digital Rebel XS camera with EOS software.

Estimation of brooding duration

We estimated brooding duration by placing 30 females with dark purple broods in a separate wells of 12-well cell culture dishes filled with artificial seawater. We checked females every 1 to 3 d to note embryo color and check for juvenile hatchlings (Supplementary material Fig. S1). Because females may have oviposited earlier than the initiation of this study, the average duration of brooding time presented here is minimal developmental time.

Improvement of artificial rearing

After removing from their marsupium, we split three broods of about 20 purple (early stage) embryos each into a control (daily hand pipette rotation) and experimental (constant shaker rotation) group, each group contained around 9 to 10 embryos. We reared all groups in 6-well culture dishes in artificial seawater at 12 °C and counted embryos daily. We identified dead embryos by their malformed morphology and removed these from their well, and calculated percent survival by dividing the number of live embryos in the group by the initial size of the group.

Brood and carapace measurements

We examined brood size, carapace size, and brood age of 91 adult females to determine whether brood size decreases with brood age (suggesting that embryos die and are removed over the course of brood development) and whether larger females are able to produce larger broods (suggesting they have more reproductive resources). We removed embryos from the female carapace as described previously, noting the approximate stage of the embryos and counting the total number of embryos per brood. One valve from each female was retained before fixation, and we photographed the valve under a dissection microscope. We measured the anteroposterior length and two-dimensional area of the carapace from the resulting photographs using ImageJ; six valves were crushed during dissection and not measured. For simplicity, we categorized brood ages as "early" (cleavage and germ band stages), "mid" (limb bud and head stages), and "late" (eye spot stage). We counted brood sizes of 30 females with early embryos, 31 broods from females with mid-stage embryos, and 30 broods of late embryos. We performed ANOVA to determine whether brood size was significantly different at different stages, and performed linear regression analysis to determine if carapace size was correlated with brood size.

RESULTS

Improvement of artificial rearing

One logistical obstacle which makes *E. carcharodonta* and other slow-developing crustaceans difficult to study is inefficient and relatively unsuccessful artificial rearing in the laboratory. To observe longer-term development of embryos, however, live embryos must be removed from a brooding female and incubated for several weeks. It is thought that rotation of the embryos is important for the survival of other brooding crustaceans (e.g., Vannier & Abe, 1993; Baeza & Fernandez, 2002; Wakayama, 2007). We thus rotated artificially reared embryos on a shaker with constant movement or by hand with a pipette. Pipette-rotated early embryos only lived for about a week while shaker-rotated embryos lived up to 28 d outside of the marsupium (Supplementary material Fig. S1. While the shaker-table treatment was not sufficient to maintain embryos throughout the entire duration of embryogenesis, embryos did show physical signs of development during the course of the experiment, allowing for study of artificially reared embryos over the course of several weeks, rather than several days.

Brood size

Brood sizes of adult females were highly variable, the smallest brood we counted was two embryos and the largest 28, although they typically ranged from 10–20 embryos. We counted the brood size for embryos of different stages to see whether brood size decreases with brood age. We found that broods of early embryos ($N = 30$) averaged 13.8 embryos per brood (min. 4, max. 28), mid-stage broods ($N = 31$) averaged 15.65 embryos per brood (5–22), and late embryo broods ($N = 30$) averaged 16.87 embryos per brood (2–26) We found no significant difference between brood sizes at different stages (ANOVA, $P = 0.087$; Supplementary material Fig. S2), suggesting that there is not significant embryo mortality under natural brooding conditions. These brood sizes are roughly similar to other myodocopids, *Vargula annecohenae* Torres & Morin, 2007, for example, has an average brood size of 12.9 (Gerrish & Morin, 2008).

We also found no significant difference between the number of embryos brooded by females of different size. We measured the anteroposterior length and total 2D area of one removed valve from 85 brooding females and found that the average anteroposterior length (or diameter) of an adult valve is 1.936 mm and the average area of the shape circumscribing the widest part of its valve (2D shape) 2.082 mm^2. While area and length are tightly associated ($R^2 = 0.89$, $P = 3.52 \times 10^{-42}$), neither was tightly associated with brood size ($R^2 = 0.017$, $P = 0.23$ and 0.016, $P = 0.25$ respectively; Supplementary material Fig. S3). This suggest that larger females do not produce larger broods.

Overview of embryogenesis

We incubated females soon after oviposition, as estimated by color of the embryos in her marsupium, in isolated dishes at 12–14°C. While some broods died during this time period, most lived and we estimate that embryogenesis in *E. carcharodonta* lasts 65–75 d from oviposition to hatching (Table 1). Because of this lengthy period, inefficient artificial rearing, and small broods, we made most of our observations by comparing several broods at different developmental timepoints, rather than by continuous observation of a single cohort.

Fertilized eggs are approximately 300–350 µm in diameter lengthwise, and 250 µm widthwise. Embryos undergo characteristic changes in appearance in amount of yolk and color of yolk (Supplementary material Figs. S1, S4). After extrusion into the marsupium, fertilized eggs are filled with yolk granules, giving them a distinctive dark purple color under top lighting (Supplementary material Fig. S1A) though they appear orange with a bottom light (Supplementary material Fig. S4A). Although we have not been able to observe females extruding eggs into their marsupium, we have observed embryos at the single nuclear stage (Fig. 1A, B). These embryos have, in addition to a large or bright nucleus, three polar nuclei that likely represent the polar bodies. These polar bodies are clearly visible until the 16-cell stage (Fig. 1A–E). Early cell divisions appeared synchronous. In embryos with dividing cells (i.e., with cells in metaphase or anaphase) all cells exhibited signs of mitotic chromosomes (Figs. 1A–G, 2A). Most nuclei

Table 1. Stages of embryos. *Color as visible by eye or under a dissection scope with top lighting; **from Wakayama (2007).

Stage	Color*	Morphology	Days	Figures	Supplementary figures	*V. hilgendorfii* days**
Cleavage	Purple	cleavage to germ disc	1-?	1A-H	2A	Days 1-?
				2A,B	4A	(early)
Germ-band	Lavender	Germ band	?-13	1I-M	2B	Days?-3
				2C	4B	(early)
Limb	Orange	Limb buds form	14–41	1N-P	2C	Days 4–5
				3A,B	4C,D	(appendage I)
Head	Orange	Anterior tissue mass grows	42–57	3C,D	2D,E	Days 6–7
				4A,C,D	4E, 5A,B	(appendage II)
Eye	Bright orange-pink	Eyespots form to hatching	58–70	3E,F	2F	Days 8–16
				4B	4F, 5C,D	(carapace repartition)

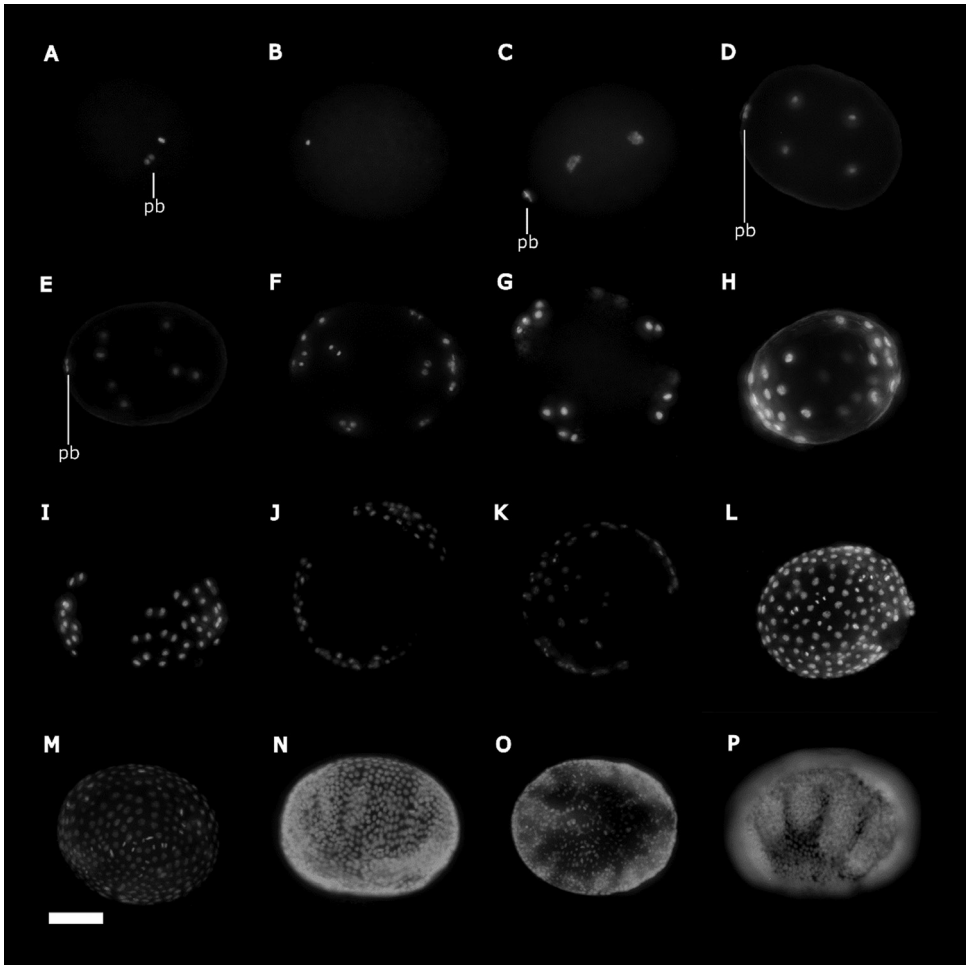

Figure 1. Early embryogenesis of *Euphilomedes carcharodonta* visualized with DAPI nuclear staining; cleavage stage (**A–M**), germ-band stage (**N, O**), limb-bud stage (**P**). A single-cell embryo with a polar body (pb) is visible on one face of embryo next to the embryonic nucleus (**A**). Another orientation of a single-cell embryo with the polar body (not visible) on the opposite side of the visible embryonic nucleus (**B**). An embryo with two-nuclei and a polar body (**C**). A four-nuclei embryo with a polar body (**D**). An eight-nuclei embryo, this is the oldest stage with an obvious polar body (**E**). In a sixteen-nuclei embryo the nuclei have moved superficially, this is the oldest stage with clearly synchronous cell divisions (**F**). After the sixteen-cell stage the nuclei are at the surface of the embryo but have not yet coalesced (**G**). Nuclei begin to coalesce in a band around the embryo with a higher concentration at the narrow poles (**H**). Nuclei continue dividing in a linear pattern (**I**), creating a band that extends medially (**J**). Nuclei begin to cover lateral surfaces, perhaps by epiboly (**K**). Nuclei continue to divide, covering the embryo (**L**), and eventually creating a semi-even layer around the yolk (**M**). The axes of the embryo become evident as the superficial nuclei begin to form undulations on the lateral sides. This is a lateral view of an early limb bud stage with anterior to the right (**N**). Ventral view of the same embryo as in (**N**), anterior is to the right (**O**). Lateral view of a later limb bud stage embryo, anterior is to the right. Limb buds are visible as lateral condensations of nuclei (**P**); pb, polar body. Scale bar =100 µm.

were clearly at the surface of the embryo in these early stages, but we were unable to observe a clear cleavage plane or furrow. The nuclei appeared to move superficially and become more evenly-spaced around the surface of the embryo after approximately 16 nuclei had formed (Fig. 3F). Cells began to divide asynchronously after this stage (Figs. 1G–P, 2B, C) then apparently migrated toward the two extreme poles of the embryo, forming rows of nuclei at each end (Fig. 1H). The nuclei then spread peripherally outward from both poles, creating linear rows wrapping around the embryo in an apparent germ band (Fig. 1I, J). The nuclei eventually appear to migrate toward the lateral surfaces, then epibolize to cover the entire yolk evenly (Fig. 1L, M). This germ band layer is thin and difficult to see under brightfield (Supplementary material Figs. S1B, S4B); embryos of this age are lavender in color.

By day 14, the yolk mass has begun to visibly shrink and become more orange in color as the surface tissue forms undulations, the future limb buds (Supplementary material Fig. S4C). While these undulations are difficult to see in brightfield, they are quite evident in DAPI-stained embryos (Fig. 1N, O). Over the next two weeks, these undulations grow into limb buds easily visible under brightfield (Fig. 1P and Supplementary material Figs. S1C, S4D). Around day 42, the anteriormost tissue begins to outpace the growth of posterior tissues to form a head region (Supplementary material Figs. S1D, E, S4E). Near the end of embryogenesis, around day 58, small red eyespots become visible as does the carapace, and limbs begin to move, the head region continues to grow during this time as the yolk shrinks (Supplementary material Figs. S1F, S4F). After approximately 65–75 d, at the end of embryogenesis, embryos tear through the chorion with their furcal claw and hatch as first instar juveniles.

Limb bud and carapace formation

The presumptive fates of the limb buds are homologized to *V. hilgendorfii* (Wakayama, 2007). Tentative assignments are given in Figure 3. We counted five cell mounds with furrows between them (undulations) before definitive limb bud formation. These

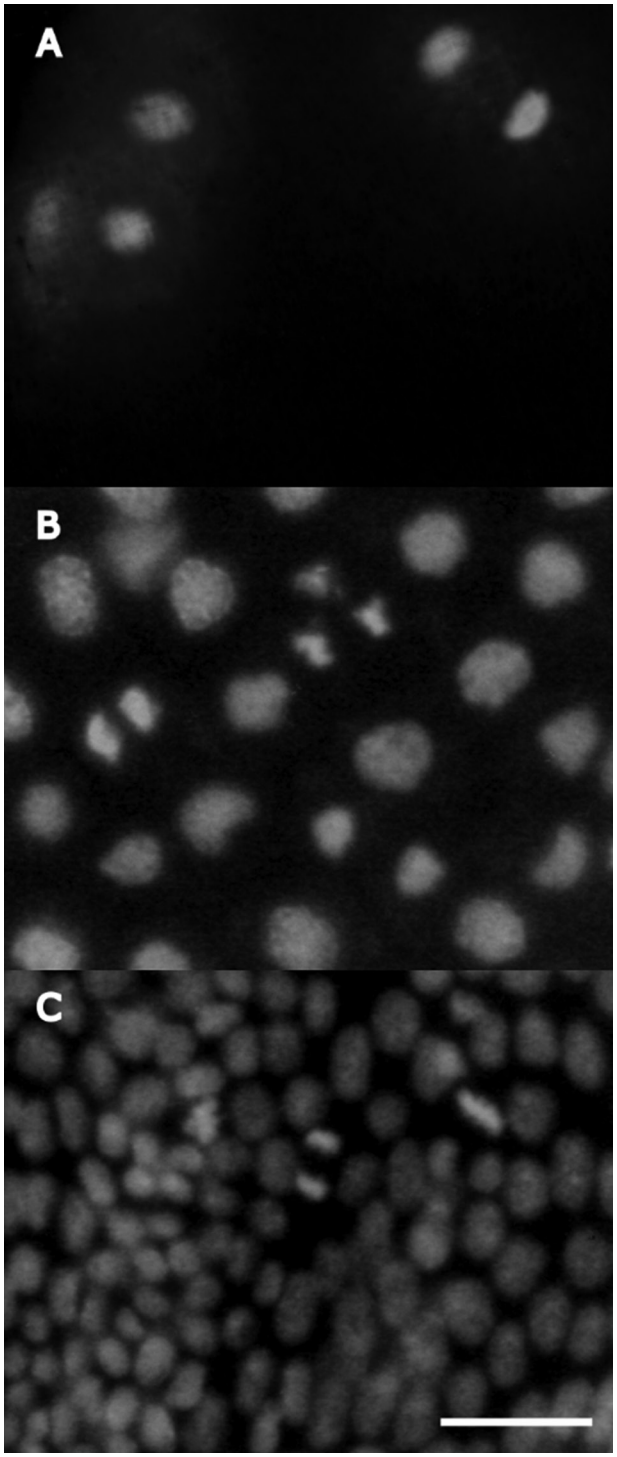

Figure 2. Asynchronous and synchronous nuclear divisions. Nuclei of cleavage and germ-band stage embryos visualized with DAPI staining. Dividing cells were identified by their appearance of metaphase or anaphase morphologies. Early divisions occurred synchronously, whereas later divisions were asynchronous. All closeups are of embryos in Figure 2. Sixteen-cell stage (Fig. 2G) with synchronous divisions (**A**). Asynchronous divisions in a late-cleavage stage embryo, same embryo as Figure 2L (**B**). Asynchronous divisions in a germ-band stage embryo, same embryo as Figure 2N and O (**C**). Scale bar = 30μm.

undulations apparently become the first five limbs: first antenna/antennule, second antenna, mandibles, maxillules, and fifth limb as well as undifferentiated posterior tissue, some of which may correspond to the furcal claw. Unlike *V. hilgendorfii*, limb bud undulations are visible long before the carapace buds become obvious. The first carapace buds we saw were not visible until head stage (day 42), while slight undulations corresponding to future limb buds were visible by day 14. The carapace begins as two buds on the dorsolateral surfaces (visible in a head stage embryo in Fig. 3C, D). As the carapace continues to develop, it grows to cover the lateral sides of the embryo during head, limb, and eye stages (Fig. 3E, F; Supplementary material Fig. S5). Evidence of a carapace furrow is evident with nuclear staining (Fig. 3C, E), but it is difficult to homologize the morphology of the developing carapace to other ostracod groups without SEM, in particular how the carapace joins and what the juncture looks like as it occurs.

Development of the central nervous system

We visualized the embryonic nervous system of *E. carcharodonta* using antibodies against acetylated-alpha tubulin, which is abundant in developing axons in arthropods (e.g., Harzsch *et al.*, 1997; Harzsch & Glötzner, 2002; Brenneis & Richter, 2010; Brenneis, 2013; Mayer *et al.*, 2013). This study represents, to our knowledge the first instance of immunohistochemical staining in an ostracod.

The embryonic brain structure of *E. carcharodonta* is typical that of crustaceans, with three distinct parts: protocerebrum, deutocerebrum, and tritocerebrum (Fig. 4A, B, D; after Harzsch, 2006 and references therein). This structure is visible by the head stage of development and perhaps even earlier, while the embryo still appears purple/lavender, well before limb bud elongation. A maximum of nine ganglia pairs were visible in the observed specimens; however, it has not yet been determined if the number of ganglia pairs are correlated with age. The ganglia appear to innervate the proximal portions of the developing limb buds, but a closer examination is necessary to confirm this (Fig. 4C).

DISCUSSION

Development of *E. carcharodonta* lasts 65–75 d, which is a much longer brooding period than in *V. hilgendorfii* (about 16 d) and about 21–30 d in other cold-water myodocopids (Cohen & Morin, 1990). While long brooding periods in *E. carcharodonta* could present a somewhat logistical challenge, this does offer insight into the developmental timing of slower-to-develop ostracods. We presented practical information for rearing slower-growing ostracods in the laboratory. We can maintain embryos on a shaker for about 30 d, nearly half of the 65–75 d total time for embryogenesis. We found no significant embryonic death for individuals naturally reared in their mother's marsupium, neither we found significant differences in brood sizes between mothers of different size. This suggests there is no benefit to selecting for larger or smaller females when setting up tanks for husbandry. It also suggests that the previously reported correlation between female size and brood size between species (Kornicker, 1981, 1986) may not extend to within-species comparison. We also presented our observations of early cleavage patterns, limb and carapace development, and the general morphology of the embryonic central nervous system.

Embryogenesis of myodocopid ostracods

The unique extreme reduction of segmentation and the bivalved carapace of ostracods make them an intriguing subject for embryological studies. *Euphilomedes carcharodonta*, a sarsielloid ostracod, shows many similarities to the fast-developing cypridinidid myodocopid, *Vargula hilgendorfii* (Wakayama, 2007; Ikuta, 2017) in that both exhibit cleavage without distinct cleavage furrows, develop their carapace as two lateral buds that later fuse to form a hinge, and develop their first five appendages simultaneously from surface undulations (Wakayama, 2007; Ikuta, 2017). Like *V. hilgendorfii*, cleavage stages in *E. carcharodonta* do not show distinct cleavage

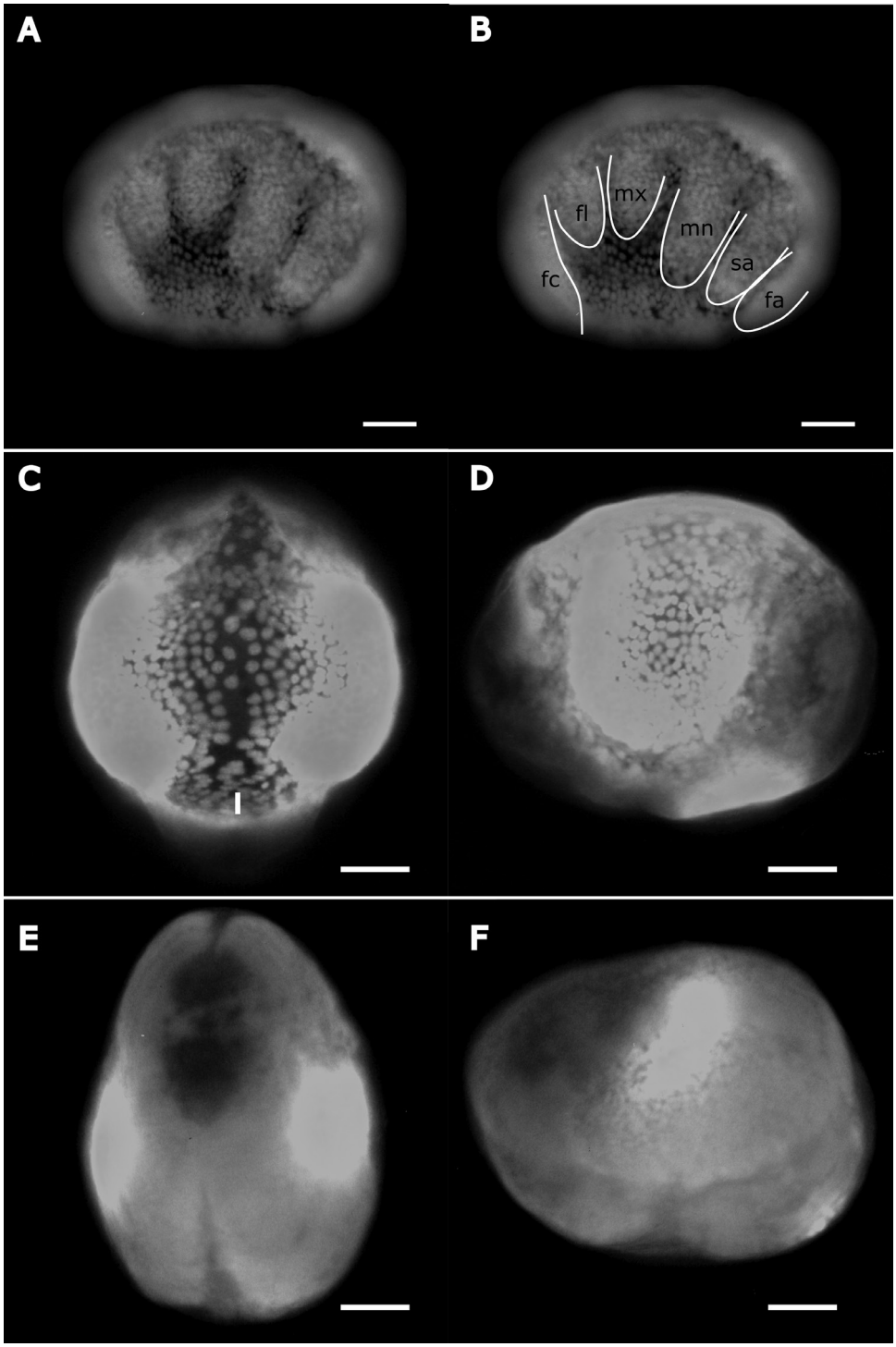

Figure 3. Limb and carapace development. Nuclei of limb through eye-stage embryos visualized with DAPI. **A** and **B** are the same embryo as in Figure 2P, with limb buds outlined in white and labelled in (**B**). Dorsal view of head-stage embryo with developing carapace, arrow points at evidence of a hinge or furrow between the two valves, anterior is up (**C**). Left lateral view of embryo from **C**, anterior is to the right (**D**). Dorsal view of eye-stage embryo, anterior is up (**E**). Left lateral view of embryo in **E (F).** Supplementary material Fig. S5 shows these embryos with carapace and limbs colorized. fa, first antenna; sa, second antenna; mn, mandible; mx, maxillule; fl, fifth limb; fc, furcal claw or undifferentiated posterior tissue. Scale bar = 100 μm.

furrows (Wakayama, 2007). This suggests that cleavage patterns may differ between Podocopa and Myodocopa, the two extant lineages of Ostracoda. Ostracod cleavage was once assumed to be holoblastic and equal, based on podocopids alone, but our work confirms that universal cleavage patterns for Ostracoda have not been clearly identified (Fig. 5; Minelli *et al.*, 2013). As ostracods are representatives of the Oligostraca, the most understudied of the three major pancrustacean clades (Oakley *et al.*, 2013), resolving the diversity and evolutionary history of their cleavage patterns will be instrumental to understanding the evolution of early development in this group (Fig. 6).

Carapace development in *E. carcharodonta* is similar to carapace development in *V. hilgendorfii*. Both build a carapace from two distinct carapace buds, a situation that differs from the one-piece

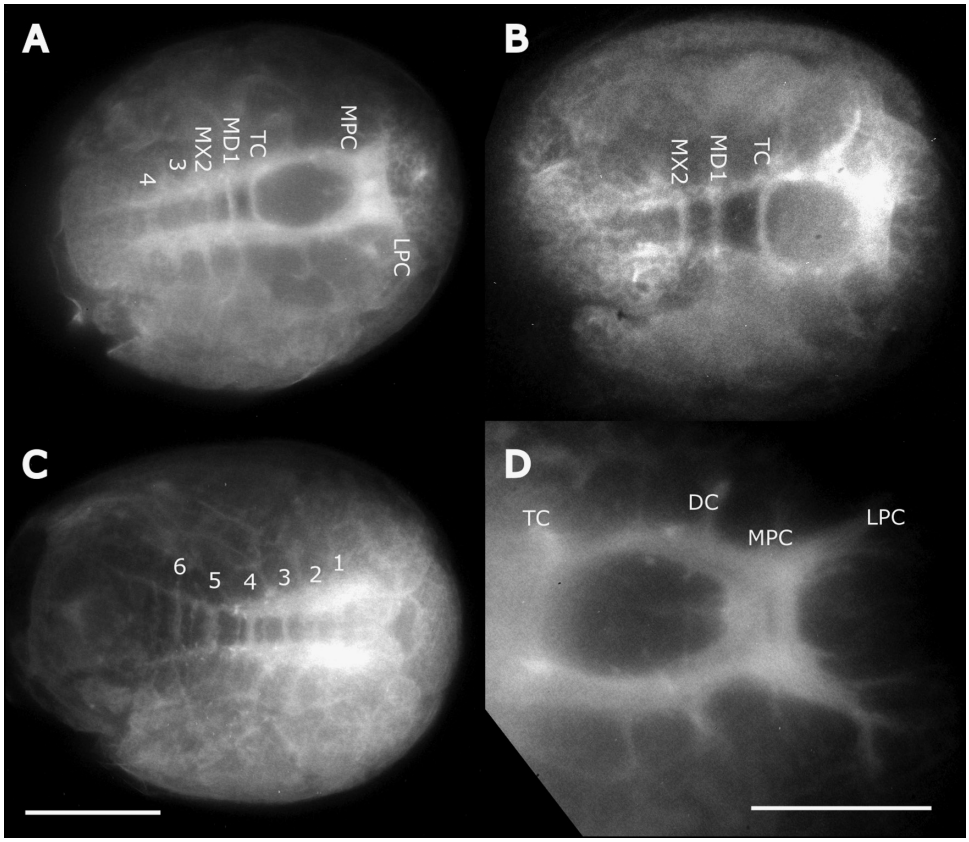

Figure 4. Development of the central nervous system. Embryos were immunostained with anti-ac-tubulin and viewed wholemount. Immunostaining results were confirmed with phalloidin staining (not shown). Head through eye-spot stage embryos showed clear circumoral rings and posterior pairs of ganglia, correspondence of ganglia to developing limb structures in uncertain, labels here are tentative. Anterior is to the right in all panels; anterodorsal view of a head stage embryo. The developing brain and first four segmental ganglia are visible (**A**). Anterodorsal view of an eye stage embryo. Due to the curvature of the embryo, only the first two posterior nervous system segments are visible (**B**). Dorsal view of head stage embryo in panel **A**. Additional posterior ganglia are visible (**C**). Head structures of head stage embryo in panels **A** and **C,** the three major parts of the brain (protocerebrum, deutocerebrum, and tritocerebrum) are clearly discernible (**D**); LPC, lateral protocerebrum; MPC, median protocerebrum; DC, deutocerebrum; TC, tritocerebrum; MD, mandibular; MX, maxillary.

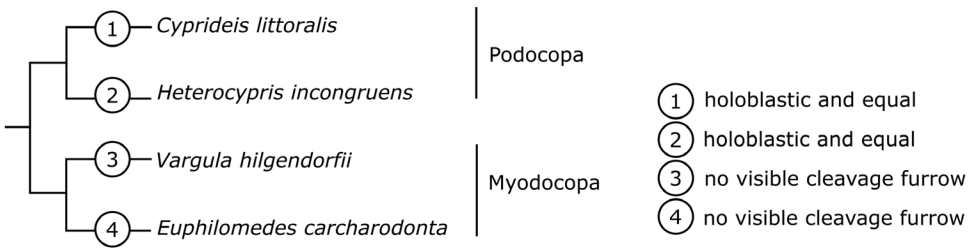

Figure 5. Cleavage patterns in Ostracoda. Summary of cleavage patterns from species previously studied. Cleavage patterns differ between Podocopa and Myodocopa, with Podocopa described as having holoblastic and equal cleavages, whereas cleavages in Myodocopa do not show evidence of a visible cleavage plane or furrow (Müller-Calé, 1913; Weygold, 1960; Wakayama, 2007). *Cyprideis littoralis* Brady, 1868 *Heterocypris incongruens* Ramdohr, 1808.

carapaces of some fossil juvenile ostracods (Hanai & Tabuki, 1995; Siveter *et al.*, 2003). Unlike *V. hilgendorfii* embryos, however, we found no evidence that *E. carcharodonta* exhibit a transient hingeless carapace stage, although a more detailed EM study with might prove otherwise (Wakayama, 2007).

The nervous system in ostracod embryos

The adult ostracod nervous system has been described in a few podocopid ostracods, where it was studied using classical histological techniques (Turner, 1896; Cannon, 1931; Weygoldt, 1960). Studies on the embryonic nervous system are even more scarce than studies of the adult nervous system, with only a single study in the last century (Weygoldt, 1960). This study followed the development of the central nervous system with an emphasis on the development of nerve ganglia. While Weygoldt (1960) provided a good starting point for understanding ostracod nervous systems, it is difficult to use as a general reference as it only has hand-drawn figures. Furthermore, as modern staining techniques become more commonplace, photographic representation of the

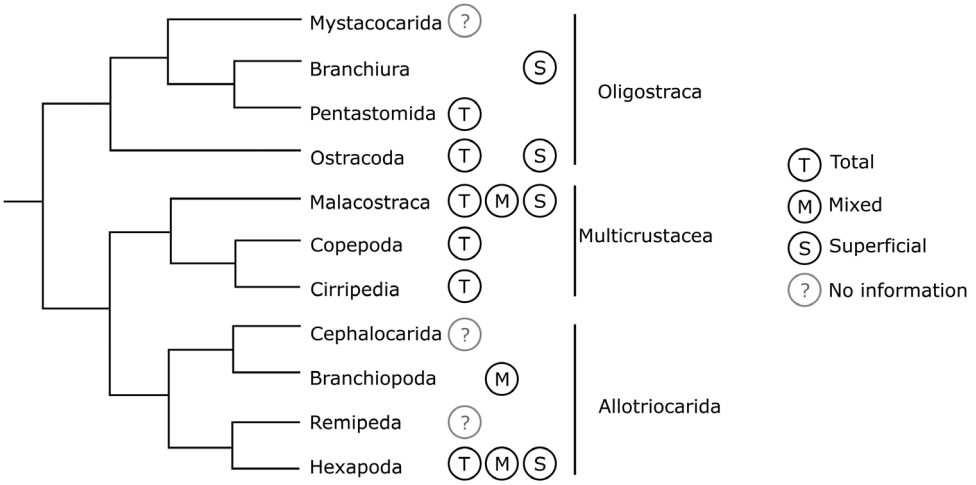

Figure 6. Cleavage patterns vary among crustacean taxa. Many lineages (e.g. Malaostraca, Ostracoda) have several cleavage patterns represented within the taxon. Several groups are missing information regarding their cleavage patterns. Names of crustacean taxa based on Oakley *et al.*, (2013).

nervous system becomes increasingly powerful as a representation of the nervous system as well as a reference for comparison.

We presented the first immunostaining of the embryonic nervous system of ostracods. It is clear that the embryonic nervous system of *E. carcharodonta* shares the general crustacean embryonic nervous system architecture. One major point of difference between *E. carcharodonta* and *Vargula* is the absence of embryonic compound eyes (Wakayama, 2007; Gerrish & Morin, 2008). Brown eye-spots arise just after limb and carapace bud formation in *V. hilgendorii*. These eyes increase in size and ommatidial number in the ensuing week, and embryos hatch with a fully-formed compound eye (Wakayama, 2007). *Euphilomedes carachrodonta* and at least one other congener, *E. morini*, form red eye-spots that do not appear to correspond with an ommatidial field after limb and carapace bud formation (Rivera & Oakley, 2009; Table 1, Supplementary material Fig. S1). These non-ommatidial eye-spots are maintained without elaboration through the first half of juvenile development, representing a major heterochronic shift in this genus (Rivera & Oakley, 2009). After the first half of juvenile development, males restart eye development and form a second (brown) eye-field that adds ommatidia during instars IV and V; this restart of eye development is associated with increased expression of eye-development genes Dachshund, Chaoptic, and Pax-2 (Sajuthi *et al.*, 2015). Our newly developed immunohistochemical methods now open the possibility of studying the nervous system changes associated with heterochronic eye development in *Euphilomedes* as well as broader questions across Ostracoda.

SUPPLEMENTARY MATERIAL

Supplementary material is available at *Journal of Crustacean Biology* online.

S1 Figure. Photographs of live embryos of *Euphilomedes carcharodonta* taken under a dissection microscope.

S2 Figure. Average percent survival for artificially reared embryos of *Euphilomedes carcharodonta*.

S3 Figure. Brood size of *Euphilomedes carcharodonta*.

S4 Figure. Overview of development of *Euphilomedes carcharodonta*.

S5 Figure. Carapace development in late embryos of *Euphilomedes carcharodonta*.

ACKNOWLEDGEMENTS

Thanks to current and former members of the Rivera laboratory for help in dissection, collection, and animal care. Special thanks to Alexis Arenz, Arvind Arul Nambi Rajan, Tiffanie Tran, Dylan Ong, Lisa Sasaki, Alyssa Kim, Erik Wictor, Solana Tong, Brian Cheng, Nathan Haberkern, Ozair (Ozzie) Ferozuddin, and Henry Le for helpful discussion and animal care. Thanks to an anonymous reviewer and Joanna Wolfe for invaluable comments on the manuscript.

REFERENCES

Arenz, A., Tran, T., Koyama, K., Gomez, A.M. & Rivera, A.S. 2018. Sexually dimorphic eye-loss driven by ecological selection in an ostracod crustacean: support for the reproductive role hypothesis. *Integrative and Comparative Biology*, **58**: 431–440.

Baeza, J.A. & Fernandez, M. 2002. Active brood care in *Cancer setosus* (Crustacea: Decapoda): The relationship between female behaviour, embryo oxygen consumption and the cost of brooding. *Functional Ecology*, **16**: 241–251.

Baltanás, A., Otero, M., Arqueros, L., Rossetti, G. & Rossi, V. 2000. Ontogenetic changes in the carapace shape of the non-marine ostracod *Eucypris virens* (Jurine). In: *Evolutionary Biology and Ecology of Ostracoda: Theme 3 of the 13th International Symposium on Ostracoda (ISO97)* (D.J. Horne & K. Martens, eds.), pp. 65–72. Springer Netherlands, Dordrecht.

Brady, G.S. 1868. On the crustacean fauna of the salt marshes of Northumberland and Durham. *Natural History Transactions of Northumberland*, **3**: 120–136.

Brenneis, G. & Richter, S. 2010. Architecture of the nervous system in Mystacocarida (Arthropoda, Crustacea) an immunohistochemical study and 3D reconstruction. *Journal of Morphology*, **271**: 169–189.

Brenneis, G., Stollewerk, A. & Scholtz, G. 2013. Embryonic neurogenesis in *Pseudopallene* sp. (Arthropoda, Pycnogonida) includes two subsequent phases with similarities to different arthropod groups. *BMC EvoDevo*, **4**: 32 [doi.org/10.1186/2041-9139-4-32].

Brusca, R.C., Moore, W. & Shuster, S.M. 2016. *Invertebrates*, Edn. 3. Sinauer, Sunderland, MA, USA.

Cannon, H.G. 1931. *On the Anatomy of a Marine Ostracod*, Cypridina (Doloria) levis *Skogsberg*. Cambridge University Press, Cambridge, UK.

Cohen, A.C. 1983. Rearing and postembryonic development of the myodocopid ostracode *Skogsbergia lerneri* from coral reefs of Belize and the Bahamas. *Journal of Crustacean Biology*, **3**: 235–256.

Cohen, A.C. & Morin, J.G. 1990. Patterns of reproduction in Ostracodes: A Review. *Journal of Crustacean Biology*, **10**: 184–211.

Ellis, E.A. & Oakley, T.H. 2016. High rates of Species Accumulation in Animals with Bioluminescent Courtship Displays. *Current Biology*, **26**: 1916–1921.

Gerrish, G.A. & Morin, J.G. 2008. Life cycle of a bioluminescent marine ostracode, *Vargula annecohenae* (Myodocopida: Cypridinidae). *Journal of Crustacean Biology*, **28**: 669–674.

Gerrish, G.A. & Morin, J.G. 2016. Living in sympatry via differentiation in time, space and display characters of courtship behaviors of bioluminescent marine ostracods. *Marine Biology*, **163**: 190–204.

Hanai, T. & Tabuki, R. 1995. Shell structure of Promanawa. Discussion on the bauplan of podocopid Ostracoda. *Mitteilungen aus dem Hamburgischen Zoologischen Museum und Institut*, **92**(Supplement): 259–272.

Harzsch, S. 2006. Neurophylogeny: Architecture of the nervous system and a fresh view on arthropod phyologeny. *Integrative and Comparative Biology*, **46**: 162–194.

Harzsch, S. & Glötzner, J. 2002. An immunohistochemical study of structure and development of the nervous system in the brine shrimp *Artemia salina* Linnaeus, 1758 (Branchiopoda, Anostraca) with remarks on the evolution of the arthropod brain. *Arthropod Structure & Development*, **30**: 251–270.

Harzsch, S., Anger, K. & Dawirs, R.R. 1997. Immunocytochemical detection of acetylated alpha-tubulin and Drosophila synapsin in the embryonic crustacean nervous system. *International Journal of Developmental Biology*, **41**: 477–484.

Horne, D.J., Smith, R.J., Whittaker, J.E. & Murray, J.W. 2004. The first British record and a new species of the superfamily Terrestricytheroidea (Crustacea, Ostracoda): morphology, ontogeny, lifestyle and phylogeny. *Zoological Journal of the Linnean Society*, **142**: 253–288.

Ikeya, N., Tsukagoshi, A. & Horne, D.J. 2005. Preface: The phylogeny, fossil record and ecological diversity of ostracod crustaceans. *Hydrobiologia*, **538**: vii–xiii.

Ikuta, K. 2017. Expression of two *engrailed* genes in the embryo of *Vargula hilgendorfii* (Muller, 1980) (Ostracoda: Myodocopina). *Journal of Crustacean Biology*, **38**: 23–26.

Kornicker, L.S. 1981. Revision, distribution, ecology, and ontogeny of the ostracode subfamily Cyclasteropinae (Myodocopina: Cylindroleberididae). *Smithsonian Contributions to Zoology*, **319**: 1–548.

Kornicker, L.S. 1986. Sarsiellidae of the Western Atlantic and Northern Gulf of Mexico, and revision of the Sarsiellinae (Ostracoda: Myodocopina). *Smithsonian Contributions to Zoology*, **415**: 1–217.

Kornicker, L.S. & Harrison-Nelson, E. 1997. Myodocopid Ostracoda of Pillar Point Harbor, Half Moon Bay, California. *Smithsonian Contributions to Zoology*, **593**: 1–53.

Kornicker, L.S. & Harrison-Nelson, E. 2002. Ontogeny of *Rutiderma darbyi* (Crustacea: Ostracoda: Myodocopida: Rutidermatidae) and comparisons with other Myodocopina. *Proceedings of the Biological Society of Washington*, **115**: 426–471.

Mayer, G., Martin, C., Rüdiger, J., Kauschke, S., Stevenson, P.A., Poprawa, I., Hohberg, K., Schill, R.O., Pflüger, H.-J. & Schlegel, M. 2013. Selective neuronal staining in tardigrades and onychophorans provides insights into the evolution of segmental ganglia in panarthropods. *BMC Evolutionary Biology*, **13**: 230 [doi: 10.1186/1471-2148-13-230].

Minelli, A., Boxshall, G. & Fusco, G. 2013. *Arthropod biology and evolution: molecules, development, morphology*, Springer, Berlin & Heidelberg.

Mueller, G.W. 1890. Neue Cypridiniden. *Zoologische Jahrbuecher Abteilung fuer Systematik Geographie und Biologie der Tiere*, **5**: 211–252.

Müller-Calé, K. 1913. Uber die Entwicklung von *Cypris incongruens*. *Zoologische Jahrbücher. Abteilung für Anatomie und Ontogenie der Tiere*, **36**: 113–170.

Oakley, T.H. 2005. Myodocopa (Crustacea: Ostracoda) as models for evolutionary studies of light and vision: Multiple origins of bioluminescence and extreme sexual dimorphism. *Hydrobiologia*, **538**: 179–192.

Oakley, T.H., Wolfe, J.M., Lindgren, A.R. & Zaharoff, A.K. 2013. Phylotranscriptomics to bring the understudied into the fold: monophyletic Ostracoda, fossil placement, and ancrustacean phylogeny. *Molecular Biology and Evolution*, **30**: 215–233.

Ramdohr, K.A. 1808. Über die Gattung Cypris Müll. und drei zu derselben gehörige neue Arten. *Magazin für die neuesten Entdeckungen in der gesammten Naturkunde der Gesellschaft naturforschender Freunde zu Berlin*, **2**: 83–93.

Rivera, A. & Oakley, T. 2009. Ontogeny of sexual dimorphism via tissue duplication in an ostracod (Crustacea). *Evolution & Development*, **11**: 233–234.

Rivers, T.J. & Morin, J.G. 2013. Female Ostracods respond to and intercept artificial conspecific male luminescent courtship displays. *Behavioral Ecology*, **24**: 877–887.

Sajuthi, A., Carrillo-Zazueta, B., Hu, B., Wang, A., Brodnansky, L. Mayberry, J. & Rivera, A.S. 2015. Sexually dimorphic gene expression in the lateral eyes of *Euphilomedes carcharodonta* (Ostracoda, Pancrustacea). *BMC EvoDevo*, **6**: 34 [doi: 10.1186/s13227-015-0026-2].

Siveter, D.J., Sutton, M.D., Briggs, D.E.G., Siveter, D.J. 2003. An ostracode crustacean with soft parts from the Lower Silurian. *Science*, **302**: 1749–1751.

Smith, R.J. & Kamiya, T. 2002. The ontogeny of Neonesidea Oligodentata (Bairdioidea, Ostracoda, Crustacea). *Hydrobiologia*, **489**: 245–275.

Smith, R.J. & Kamiya, T. 2005. The ontogeny of the entocytherid ostracod *Uncinocythere occidentalis* (Kozloff & Whitman, 1954) Hart, 1962 (Crustacea). *Hydrobiologia*, **538**: 217–229.

Smith, V.Z. 1952. Further Ostracoda of the Vancouver Island region. *Journal of the Fisheries Research Board of Canada*, **9**: 16–41.

Speiser, D.I., Lampe, R.I., Lovdahl, V.R., Carrillo-Zazueta, B., Rivera, A.S. & Oakley, T.H. 2013. Evasion of predators contributes to the maintenance of male eyes in sexually dimorphic *Euphilomedes* ostracods (Crustacea). *Integrative and Comparative Biology*, **53**: 78–88.

Torres, E. & Morin, J.G. 2007. *Vargula annecohenae*, a new species of bioluminescent ostracode (Myodocopida: Cypridinidae) from Belize. *Journal of Crustacean Biology*, **27**: 649–659.

Turner, C.H. 1896. Morphology of the nervous system of cypris. *Journal of Comparative Neurology*, **6**: 20–44.

Turpen, J. B. & Angell, R.W. 1971. Aspects of molting and calcification in the ostracod Heterocypris. *Biological Bulletin*, **140**: 331–338.

Vannier, J. & Abe, K. 1993. Functional morphology and behavior of *Vargula hilgendorfii* (Ostracoda: Myodocopida) from Japan, and discussion of its crustacean ectoparasites: preliminary results from video recordings. *Journal of Crustacean Biology*, **1**: 51–76.

Wakayama, N. 2007. Embryonic development clarifies polyphyly in ostracod crustaceans. *Journal of Zoology*, **273**: 406–413.

Walston, T. & Hardin, J. 2010. An agar mount for observation of *Caenorhabditis elegans* embryos. *Cold Spring Harbor Protocols*, **2010** [doi:10.1101/pdb.prot5540].

Weygoldt, P. 1960. Embryologische Untersuchungen an Ostrakoden: Die Entwicklung von *Cyprideis litoralis* (G.S. Brady) (Ostracoda, Podocopa, Cytheridae). *Zoologische Jahrbucher. Abteilung für Anatomie und Ontogenie der Tiere*, **78**: 369–426.